



**A Hilbert-Huang Transform-Based  
Analysis of Heterogeneities  
from Borehole Logs**





# **A Hilbert-Huang Transform-Based Analysis of Heterogeneities from Borehole Logs**

**Said Gaci**

Sonatrach, Division Exploration, Boumerdès, Algeria. Email: [said\\_gaci@yahoo.com](mailto:said_gaci@yahoo.com)

## ***Summary***

The multi-scale nature in geophysical borehole data reflect geological heterogeneities in the Earth's crust, and cannot completely be captured with the analysis conventional methods. In this paper, a novel approach based on Hilbert-Huang transform (HHT), which combines the empirical mode decomposition (EMD) and Hilbert transform, is proposed to estimate the local scaling parameter of well log data.

The suggested method has been validated on velocity logs measured at the KTB main borehole drilled for the German Continental Deep Drilling program. The analysis of the obtained depth-varying scaling parameter allowed to identify the lithological discontinuities within the logged depth interval, and helps to quantify the complexity of crustal heterogeneities.

This new approach is of a high interest for investigating multi-scale features of the logs data, and has to be checked on large datasets to draw the possible relation between the local scaling parameter and lithology.

## 8.1 Introduction

Well logging allows to explore the evolution of petrophysical properties with depth and thus to characterize subsurface heterogeneities. An exhaustive analysis of logs is recommended to extract the maximum features of the investigated geological medium. Since well logs exhibit nonlinear and non-stationary nature, their analysis cannot be carried out using the conventional tools. That calls techniques taking into account the multi-scale features of such data, like Hilbert-Huang transform (HHT).

The HHT method was widely used as a nonlinear signal processing tool in diverse research areas (Huang and Attoh-Okine, 2005; Huang and Shen, 2005; Yan and Gao, 2007), such as analyzing seismic data in geophysics (Battista et al. 2007; Loh et al., 2001), analyzing waves and currents in oceanography (Hwang, et al. 2003), biomedical signal processing (Wu and Huang, 2009), power system quality studies (Senroy et al., 2007), etc.

For recall, HHT, introduced by Huang et al. (1998), is the combination of the Empirical Mode Decomposition (EMD) and the application of Hilbert transform to extract time-frequency information from a nonlinear and non-stationary signal. Unlike the Fourier and wavelet transforms using a priori selection of basis functions, EMD decomposes a signal into finite basis functions called the Intrinsic Mode Functions (IMFs); each IMF has a mean frequency. The analysis of the exponential law between the mean frequency and the IMF index allows computing a scaling parameter ( $\rho$ ). That offers a suitable approach to describe the multi-scale properties of the signal and to quantify its complexity. Being a global scaling parameter, it fails to locally describe the variation of the multi-scales behavior of the signal. Based on HHT-based estimation of the weighted mean frequency is suggested by Xie and Wang (2006), a new technique is proposed for

estimating the local scaling parameter, and validated on borehole logs.

The remainder of this paper is organized as follows. Section 2 gives the theory of the HHT and the details of the suggested technique. Then, the geological setting of the KTB drilling site is presented in section 3. Afterwards, section 4 presents the discussion of the results obtained by the proposed method on the KTB velocity logs. Finally, the conclusion and the perspectives of our research are detailed in section 5.

## 8.2 Theory

In this section, we propose a novel method based on the Hilbert-Huang transform (HHT) to analyze well logs. The HHT is a combination of the Empirical Mode Decomposition (EMD) and Hilbert transform (HT).

The first step of the HHT is the EMD with which the data can be decomposed into a finite number of Intrinsic Mode Functions (IMF). Each IMF satisfies two conditions:

- (1) In the whole data set, the number of local extrema and the number of zero-crossings must either equal or differ at most by one;
- (2) The running mean value of the envelope defined by the local maxima and the envelope defined by the local minima is zero.

Based on the decomposition (or shifting) process (detailed in previous chapter), the original signal  $X(z)$  is exactly reconstructed by a linear superposition of  $n$  IMFs and one residual  $r_n(z)$  :

$$X(z) = \sum_{m=1}^n \text{IMF}_m(z) + r_n(z) \quad (1)$$

The second step of the HHT consists of applying the Hilbert transform on each IMF component

$$H[\text{IMF}_m(z)] = \frac{1}{\pi} PV \int_{-\infty}^{\infty} \frac{\text{IMF}_m(\tau)}{z - \tau} d\tau \quad (2)$$

PV denotes the Cauchy principal value of this integral. An analytic signal is defined as:

$$y_m(z) = \text{IMF}_m(z) + jH[\text{IMF}_m(z)] = a_m(z) \cdot e^{j\theta_m(z)} \quad (3)$$

Where  $j = \sqrt{-1}$ ,  $a_m(z) = \sqrt{(\text{IMF}_m(z))^2 + (H[\text{IMF}_m(z)])^2}$  is the instantaneous amplitude, and  $\theta_m(z) = \tan^{-1}\left(\frac{H[\text{IMF}_m(z)]}{\text{IMF}_m(z)}\right)$  is the instantaneous phase function of the  $m^{\text{th}}$  IMF.

The instantaneous wavenumber for each IMF can be obtained by differentiating the phase:

$$\omega_m(z) = \frac{1}{2\pi} \frac{d\theta_m(z)}{dz} \quad (4)$$

Since both amplitude and frequency are functions of the spatial position  $z$ , we can present the frequency-space (or time) distribution of amplitude (or energy, the square of amplitude). This joint distribution is designated as Hilbert amplitude spectrum  $H(\omega, z)$  or simply Hilbert spectrum.

The original signal can be represented as (excluding the residual  $r_n(z)$ )

$$X(z) = RP \sum_{m=1}^n a_m(z) \cdot e^{j\theta_m(z)} = RP \sum_{m=1}^n a_m(z) \cdot e^{j \int \omega_m(z) dz} \quad (5)$$

where RP means real part.

The IMFs are treated as the basis vectors representing the data. Each basis is characterized by a different mean wavenumber ( $k_m$ ), which is inversely proportional to the characteristic scale, given by

$$k_m = \frac{\int_0^{\infty} k S_m(k) dk}{\int_0^{\infty} S_m(k) dk} \quad (6)$$

where  $S_m(k)$  is the Fourier spectrum of  $m^{\text{th}}$  IMF mode (IMF $_m$ ). It is an energy weighted mean wavenumber in the Fourier power spectrum (Huang et al., 1998).

Alternatively, another HHT-based estimation of the weighted mean wavenumber is suggested by Xie and Wang (2006):

$$k_m = \frac{\sum_{z=0}^Z \omega_m(z) a_m^2(z)}{\sum_{z=0}^Z a_m^2(z)} \quad (7)$$

where  $Z$  is the total depth.

The mean wavenumber  $k_m$  varies exponentially with the mode number  $m$  of the IMF:

$$k_m = k_0 \rho^{-m} \quad (8)$$

where  $k_0$  is a constant and  $\rho$  is the slope of the straight line fitting the  $\log(k_m)$ - $m$  graph. This illustrates that EMD acts as a dyadic filter bank in the wavenumber domain as shown by applications on stochastic simulations of fractional

Gaussian noise (fGn) (Flandrin and Goncalv ̇s, 2004; Flandrin et al., 2004), and white noise (Wu and Huang, 2004). In addition, it is expected that the  $\rho$  value is very close to 2 for such stochastic noise data. The  $\rho$  value is related to the number of scales characterizing the different modes resulting from EMD. The smaller the  $\rho$  value, the higher the number of these characteristic scales. Therefore,  $\rho$  value can be used to describe the complexity of the signal.

Since this parameter is a global measure, it doesn't allow the local study of the multi-scales features of the signal. To get rid of this shortcoming, we suggest a new approach to estimate the  $\rho$  value at each position  $z$  ( $\rho(z)$ ):

$$k_m(z) = k_0 \rho(z)^{-m} \tag{9}$$

where the weighted mean wavenumber  $k_m(z)$  is computed using the relation (7) within a moving L-length-window centred in  $z$ :

$$k_m(z) = \frac{\sum_{\tau=z-L/2}^{z+L/2} \omega_m(\tau) a_m^2(\tau)}{\sum_{\tau=z-L/2}^{z+L/2} a_m^2(\tau)} \tag{10}$$

It is worth noting that the choice of L value is of high importance. A low value leads to a rough scaling  $\log \rho(z)$  difficult to interpret, while a high value can over-smooth all the fine details of this logs. In this paper, it is determined after tests.

### 8.3 Geological Setting

The analyzed log data are recorded at the main borehole (HB, 9.1km) drilled for the German Continental Deep Drilling Program (KTB, Kontinentales

Tiefbohrprogramm). This well is located in south-eastern Bavaria (Oberpfalz, Germany), and crosses the crystalline metamorphic rocks of a Hercynian continental collision zone (Figure 1).

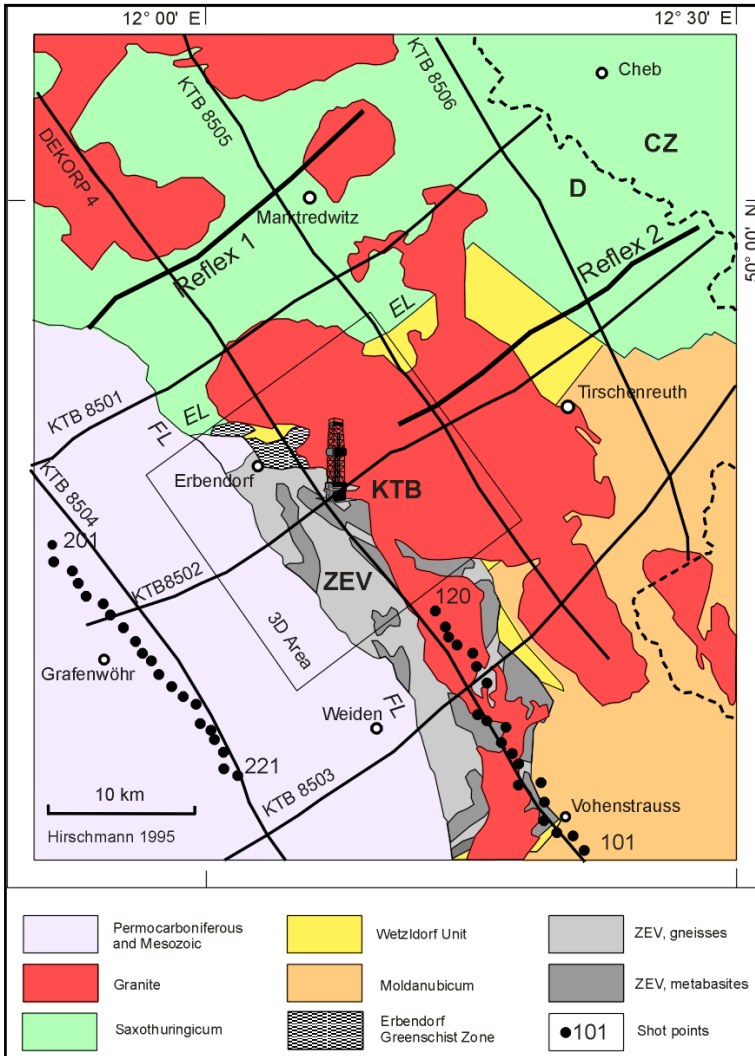


**Figure 1.** Location map of KTB borehole and main geological units of the studied area (after Harjes et al., 1997).

From the lithological point of view, the drilled section is dominated by

paragneisses, metabasites, and alternations of gneiss and amphibolite. The studied area shows the presence of many faults, cataclastic shear zones, aplitic and lamprophyric dikes (Weber and Vollbrecht, 1989) (Figure 2).

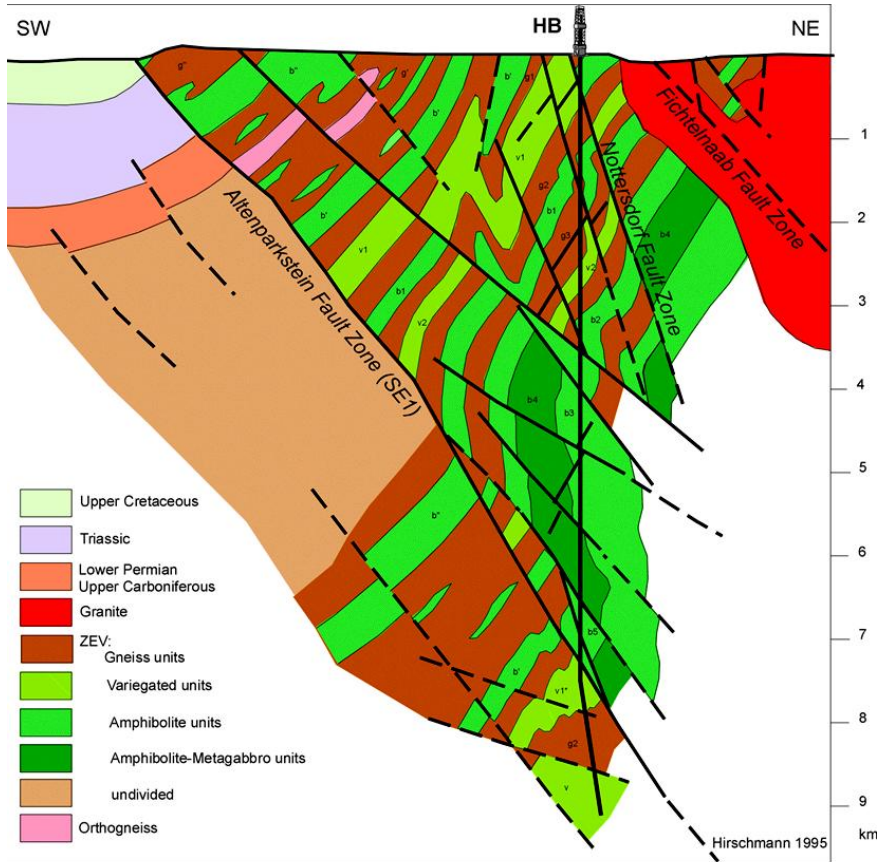


*Figure 2. Structural model in the neighbourhood of KTB well (after Hirschmann, 1996 a et b).*

## 8.4 Application on the KTB Velocity Logs

This section is devoted to the presentation and discussion of the results obtained by the suggested algorithm to explore heterogeneities from the P-wave

velocity ( $V_p$ ) and S-wave velocity ( $V_s$ ) logs recorded at the main KTB borehole. Both the logs are measured in the depth interval (290.017-4509.97m) with a minimum sampling interval of 0.1524 m (Figure 3).

As mentioned in section 2, the implementation of the suggested algorithm needs the application of the Hilbert-Huang transform (HHT) to the well logs. First, using the EMD,  $V_p(z)$  and  $V_s(z)$  are decomposed into 12 and 11 IMFs, respectively, with one residue (Figures 4-5). Then, the HHT is performed on the resulting IMFs corresponding to each velocity log, and the corresponding Hilbert amplitude spectra are presented in Figure 6. Afterwards, the relations (9) and (10) are used to evaluate the local scaling, logs,  $\rho_p(z)$  and  $\rho_s(z)$ , from the respective velocity logs  $V_p(z)$  and  $V_s(z)$  (Figure 7) using a window length  $L= 6.096$  m determined after tests.

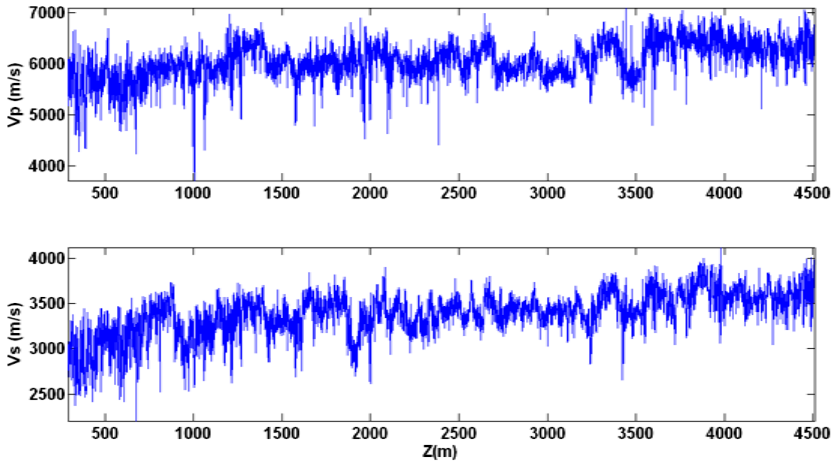


**Figure 3.**  $V_p(z)$  and  $V_s(z)$  velocity logs recorded at the main KTB borehole.

The analysis of the mean wavenumber of each IMF mode obtained from both velocity logs indicated that the EMD method acts as a filter bank  $k_m(z) \propto \rho(z)^{-m}$ . This result implies that the mean wavenumber of a given mode

is  $\rho$  times larger than the mean wavenumber of the next one. It is noticed that the local  $\rho$  values derived from both velocity logs are generally greater than 2, which would correspond to a dyadic filter bank, as reported for white noise (Wu and Huang, 2004), fractional Gaussian noise (Flandrin and Gonçalves, 2004; Flandrin et al., 2004) and turbulence time series (Huang et al., 2008). However, it still indicates that the EMD method acts as a filter bank.

The analysis of  $\rho$  value allows to draw valuable information regarding the complexity of the studied signals. Its value is inversely proportional to the number of scales involved in the EMD decomposition of the signal. A small  $\rho$  value reflects a high complexity degree of the signal.

From Figure 7, it can be noted that the complexity degree computed from the velocity logs varies with depth, and both local  $\rho$  logs exhibit a similar behavior showing a correlation coefficient of 0.74.

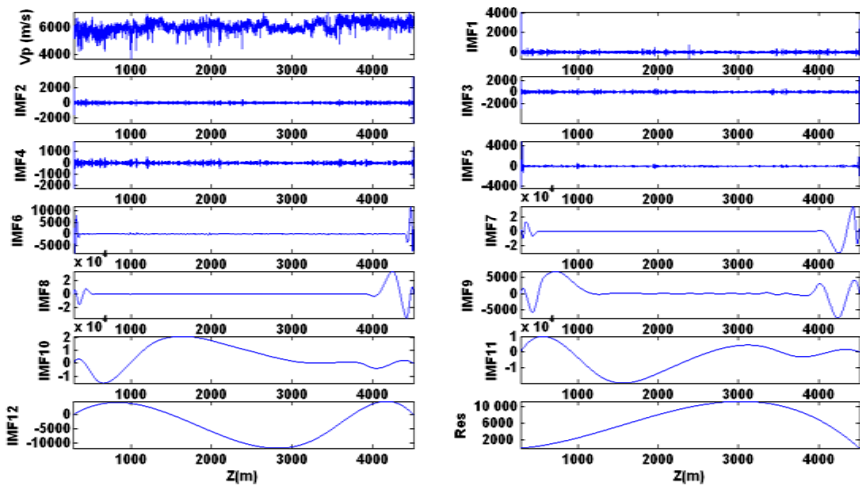


**Figure 4.** From top to bottom:  $V_p(z)$  log recorded at the main KTB borehole, 12 IMFs and residue resulting from EMD (given in m/s).

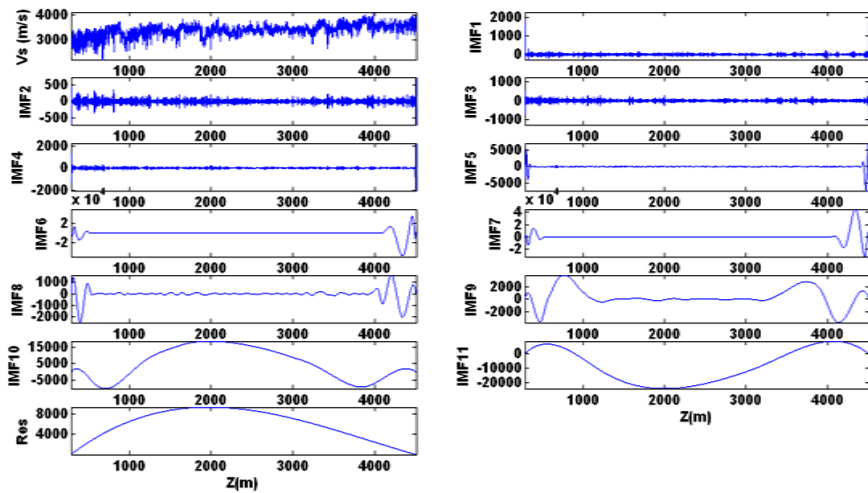
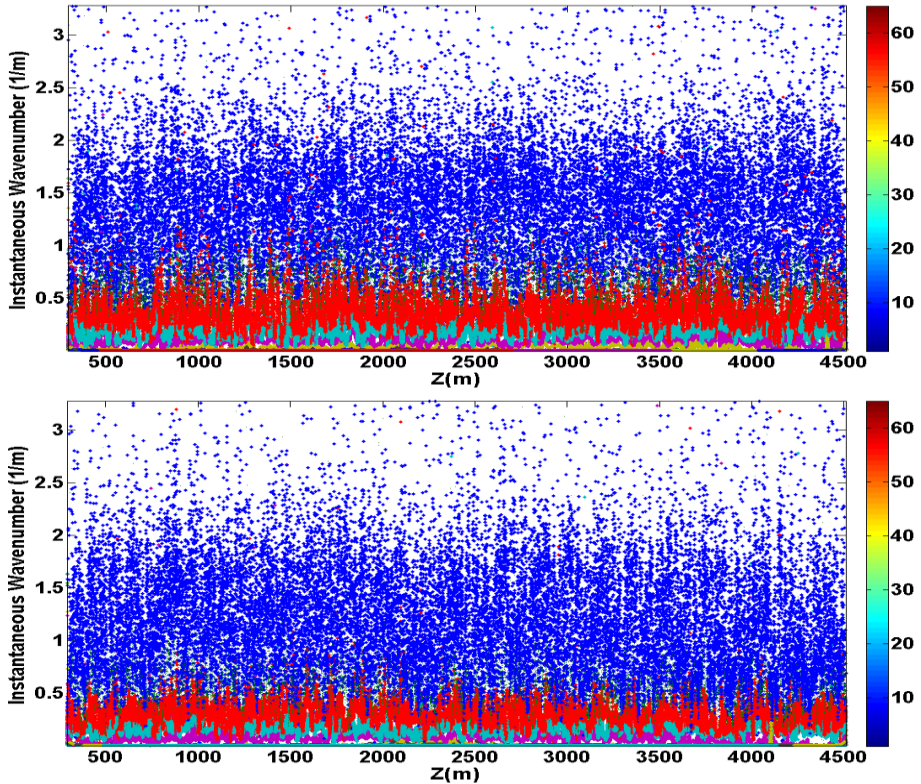
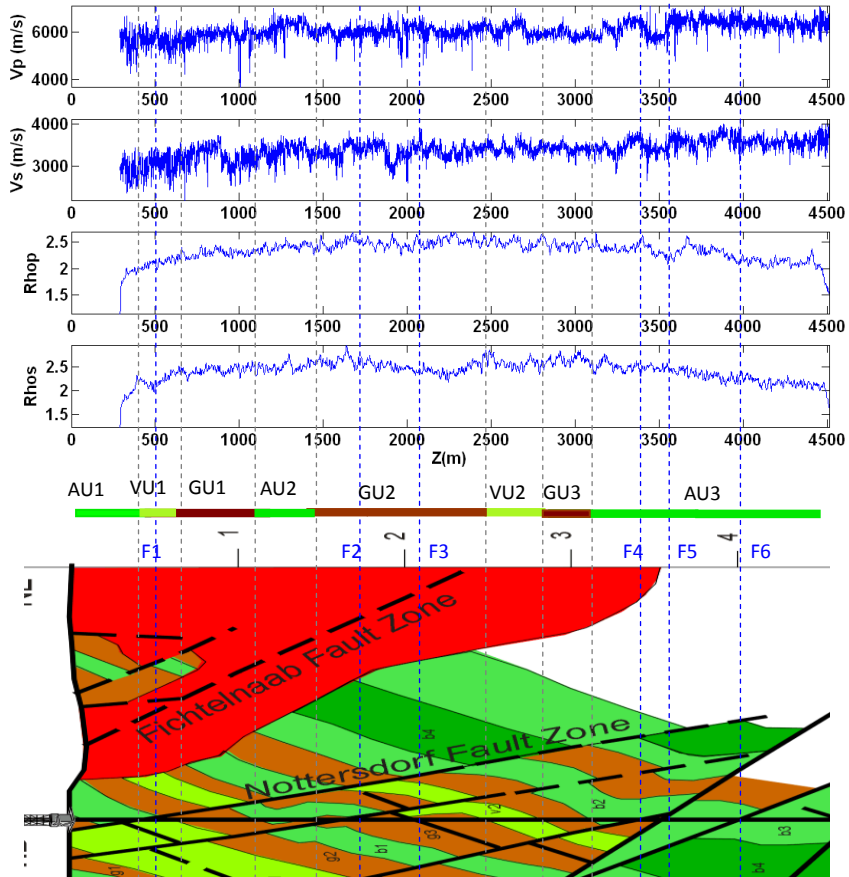


Figure 5. From top to bottom:  $V_s(z)$  log recorded at the main KTB borehole, 11 IMFs and residue resulting from EMD (given in m/s).



**Figure 6.** Hilbert amplitude spectrum of velocity logs  $V_p(z)$  (top) and  $V_s(z)$  (bottom) recorded at the main KTB borehole. The amplitude is expressed in m/s.

Using a geological section crossing the KTB borehole, a lithological segmentation is carried out on the local scaling logs. The changes of the resulted  $\rho$  value allow to put in evidence: (i) the lithological units intersected by the well (shown in gray line): AU1-AU2-AU3 (for amphibolite units), VU1-VU2 (for variegated units), and GU1-GU2-GU3 (for gneiss units), (ii) the six faults: F1-F6 (shown in blue line).



**Figure 7.** Results of the lithological segmentation obtained from the velocity logs recorded at the main KTB borehole. From top to bottom: velocity logs  $V_p(z)$  and  $V_s(z)$ , local changes of  $\rho$  value derived from those logs ( $\rho_P(z)$  and  $\rho_S(z)$ ), and a geological section crossing the KTB borehole (the lithologic sketch modified from <http://www-icdp.icdp-online.org/sites/ktb/images/Schnitt.gif>).

Blue line: faults contacts; grey line: lithological changes.

One can remark that the interfaces between the identified geological units correspond to jumps in the estimated  $\rho$  value. Other in-between sudden variations of the  $\rho$  value can be observed, which may be due to local lithological changes within these main units.

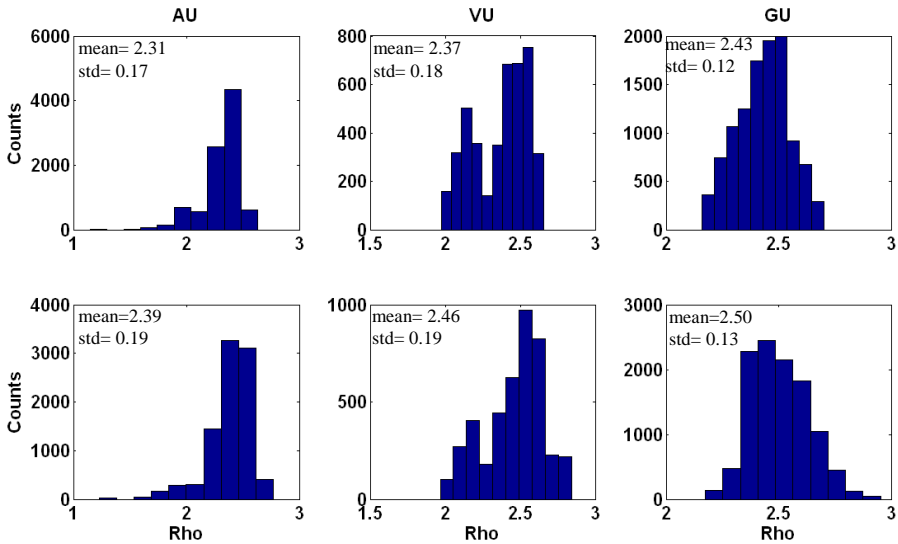


**Figure 8.** Histograms of the local  $\rho$  values corresponding to the identified lithological units crossed by the main KTB borehole.

AU: amphibolite units, VU: variegated units, and GU: gneiss units.

The histograms of the local  $\rho$  values obtained from the velocity logs show normal distributions (Figure 8). The values of the computed statistical parameters (the means and the standard-deviations) derived from these distributions, related to all the lithological units (AU, VU and GU), differ slightly. The  $\rho$  values resulted from  $V_p$  log vary from 1.1484 to 2.6330 for AU, 1.97 to 2.65 for VU and 2.16 to 2.70 for GU, while those obtained from  $V_s$  logs are between 1.23 and 2.77 for AU, between 1.97 and 2.84 for VUs, and between 2.17 and 2.95 for GU. In addition, for  $V_p$  log, the respective estimated means  $\rho$  values are 2.31, 2.37, and 2.43 for AU, VU, and GU, while for the second log, the values are 2.39, 2.46, and 2.50. The mean  $\rho$  value cannot, therefore, be used to describe a specific lithology.

Our findings show that the suggested algorithm may be of a high importance for identifying lithological discontinuities (facies changes, faults, etc.) from the variation of the estimated  $\rho$  values. Each discontinuity is marked on the scaling

log by a  $\rho$  value jump. Despite the strong correlation existing between heterogeneities and  $\rho$  value variations, a given lithology is not characterized by a unique  $\rho$  value, and the different lithologies intersected by the well exhibit very close  $\rho$  values.

## 8.5 Conclusion

In this work, we suggested a new technique based on the Hilbert-Huang transform (HHT) to analyze well logs using the depth-dependent scaling parameter ( $\rho$ ).

The potential of this method has been demonstrated by an application on real velocity logs recorded at the main KTB borehole. The variation of the obtained local  $\rho$  value allowed to perform a lithological segmentation.

The suggested technique can be considered as a new tool for evidencing lithological discontinuities by the use of the estimated scaling log. An extended application on a large survey of data is needed to give a significance of the  $\rho$  parameter value in terms of lithology.

## References

- [1] Battista, B. M., Knapp, C., McGee, T. and Goebel, V., 2007. Application of the empirical mode decomposition and Hilbert-Huang transform to seismic reflection data. *Geophysics (Society of Exploration Geophysicists)*, 72 (2), H29-H37.
- [2] Flandrin, P. and Gonçalves, P., 2004. Empirical mode decompositions as data driven wavelet-like expansions, *Int. J. Wavelets, Multires. Info. Proc.*, 2, 477-496.
- [3] Flandrin, P., Rilling, G., and Gonçalves, P., 2004. Empirical mode decomposition as a filter bank, *IEEE Sig. Proc. Lett.*, 11, 112-114.
- [4] Harjes, H.-P., Bram, K., Dürbaum, H.-J., et al., 1997. Origin and nature of crustal

- reflections: Results from integrated seismic measurements at the KTB super-deep drilling site, *J. Geophys. Res.*, 102(B8), 18267-18288.
- [5] Hirschmann, G., 1996a. KTB-The structure of a Variscan terrane boundary: seismic investigation -drilling - models. *Tectonophysics*, 264, 327-339.
- [6] Hirschmann, G., 1996b. Ergebnisse und Probleme des strukturellen Baues im Bereich der KTB Lokation. *Geologica Bavarica*, 101, 37-51.
- [7] Huang, N. E., Shen, Z., Long, S. R., Wu, M. C., Shih, E. H., Zheng, Q., Tung, C. C. and Liu, H. H., 1998, The empirical mode decomposition method and the Hilbert spectrum for non-stationary time series analysis, *Proc. Roy. Soc. London* 454A, 903-995.
- [8] Huang, N. E., and Attoh-Okine, N. O. 2005. *The Hilbert-Huang transform in Engineering*. CRC Press.
- [9] Huang, N. E., and Shen, S. S. 2005. *Hilbert-Huang transform and its applications*. World Scientific Pub Co Inc.
- [10] Huang, Y., Schmitt, F. G., Lu, Z., Liu, Y., 2008. An amplitude-frequency study of turbulent scaling intermittency using hilbert spectral analysis. *Europhys. Lett.* 84, 40010.
- [11] Hwang, P. A., Huang, N. E., and Wang, D. W., 2003. A note on analyzing nonlinear and nonstationary ocean wave data. *Applied Ocean Research (Elsevier)*, 25 (4), 187-193.
- [12] Loh, C. H., Wu, T. C. and Huang, N. E., 2001. Application of the empirical mode decomposition-Hilbert spectrum method to identify near-fault ground-motion characteristics and structural responses. *Bulletin of the Seismological Society of America (Seismol Soc America)*, 91 (5), 1339-1357.
- [13] Senroy, N., Suryanarayanan, S., and Ribeiro, P. F., 2007. An improved Hilbert--Huang method for analysis of time-varying waveforms in power quality. *Power Systems, IEEE Transactions on (IEEE)*, 22 (4), 1843-1850.
- [14] Xie, H., and Wang, Z., 2006. Mean frequency derived via Hilbert-Huang transform with application to fatigue EMG signal analysis, *computer methods and programs in biomedicine* 82, 114-120.

- [15] Yan, R., and Gao, R. X., 2007. A Tour of the Tour of the Hilbert-Huang Transform: An Empirical Tool for Signal Analysis. *Instrumentation & Measurement Magazine, IEEE (IEEE)*, 10 (5), 40-45.
- [16] Weber, K. and Vollbrecht, A., 1989. The crustal structure at the KTB drill site, Oberpfalz, in: *The German Continental Deep Drilling Program (KTB)*, edited by: Emmermann, R. and Wohlenberg, J., Springer-Verlag, Inc.
- [17] Wu, Z. and Huang, N. E., 2004. A study of the characteristics of white noise using the empirical mode decomposition method, *P. Roy. Soc. A-Math. Phys.*, 460, 1597-1611.
- [18] Wu, Z., and Huang, N. E., 2009. Ensemble Empirical Mode Decomposition: a noise-assisted data analysis method. *Advances in Adaptive Data Analysis (World Scientific Publishing Company)*, 1 (1), 1-41.

